Supplementary Information on

Neutron Scattering Studies of spin excitations in hole-doped $Ba_{0.67}K_{0.33}Fe_2As_2$ superconductor

Chenglin Zhang, Meng Wang, Huiqian Luo, Miaoyin Wang, Mengshu Liu, Jun Zhao, D. L. Abernathy, T. A. Maier, Karol Marty, M. D. Lumsden, Songxue Chi, Sung Chang, Jose A. Rodriguez-Rivera, J. W. Lynn, Tao Xiang, Jiangping Hu, Pengcheng Dai

In this supplementary information, we present raw data and discuss experimental details. The instrumentation setup and description for ARCS at spallation neutron source can be found at http://www.sns.gov/instruments/SNS/ARCS/ and MACS at NIST center for neutron research is described in ref. 1. Figure SI1 shows the temperature and wave vector dependence of the scattering at E = 3 meV. Similar to data at E = 1.5, 4, 5, and 6 meV (Figs. 1-4), we find a clean spin gap at L = even and narrowing of the Q-width along the (H, 0, L) L = odd direction. Figure SI2a shows c-axis modulations of the E = 5 meV excitations obtained on MACS. To test the spin excitation anisotropy in the in-plane moment space, we cut the ARCS data in Figs. 4a-4d along the (H,0) and (1,K) directions below and above T_c. For energy transfers below the resonance, while the scattering profile along the (H,0) direction clearly narrows below T_c (Fig. SI2b), it remains essentially unchanged along the (1,K) direction (Fig. SI2c). At the resonance energy, we find that superconductivity has no influence on the wave vector dependence of the scattering (Figs. SI2d and SI2e). Figure SI3 summarizes the temperature dependence of the (H,0,1) scattering at E = 4 meV obtained on MACS. Similar data at E = 6 meV are shown in Fig. SI4.

To quantitatively demonstrate the effect of electron- and hole-doping to the line shape of the spin excitations, we have carried out calculations using the random phase approximation (RPA) and the three-dimensional five-orbital tight-binding model obtained in Ref. [42] from fits of the DFT band structure for $BaFe_2As_2$. Figures **SI5** and **SI6** show intensity maps of the calculated in-plane spin susceptibility $\chi''(Q,\omega)$ at a fixed energy E = 15 meV for wave-vectors around Q_{AFM} for a 35% hole-doped system (Fig. SI5) and an 8% electron-doped system (Fig. SI6). The calculation is based on a RPA for the three-dimensional five-orbital tight-binding model introduced in Ref. 42 for $BaFe_2As_2$. The RPA spin susceptibility $\chi(\mathrm{Q},\omega) = \frac{1}{2}\sum_{\mathrm{l}_1,\mathrm{l}_2} \chi^{\mathrm{RPA}}_{\mathrm{l}_1\mathrm{l}_1\mathrm{l}_2\mathrm{l}_2}(\mathrm{Q},\omega)$ is obtained from the RPA multi-orbital susceptibility matrix $\chi^{\mathrm{RPA}}_{\mathrm{l}_1\mathrm{l}_1\mathrm{l}_2\mathrm{l}_2}$, which is related to the bare (Lindhard) susceptibility matrix $\chi^{0}_{\mathrm{l}_1\mathrm{l}_1\mathrm{l}_2\mathrm{l}_2}(\mathrm{Q},\omega)$ and the interaction parameters through $\chi^{\mathrm{RPA}}(\mathrm{Q},\omega) = \chi^0(\mathrm{Q},\omega)[1 - U^s\chi^0(\mathrm{Q},\omega)]^{-1}$. Here U^s is the interaction matrix in orbital space in the spin channel defined in Ref. 42 and contains on-site matrix-elements for the intra- and inter-orbital Coulomb repulsions U and U', and for the Hunds-rule coupling and pair-hopping terms J and J'. For this calculation we have used spin-rotationally invariant parameters $U'=U-2J$ and $J' = J$ with U = 0.8 eV and J = 0.2 eV. The longitudinal and transverse shape anisotropies in the hole- and electron-doped cases, respectively, can clearly be seen and are similar to what has been observed in the experiments.

SI References:

1. Rodriguez, J. A. *et al.*, MACS- a new high intensity cold neutron spectrometer at NIST, *Meas. Sci. Technol.* **19**, 034023 (2008).

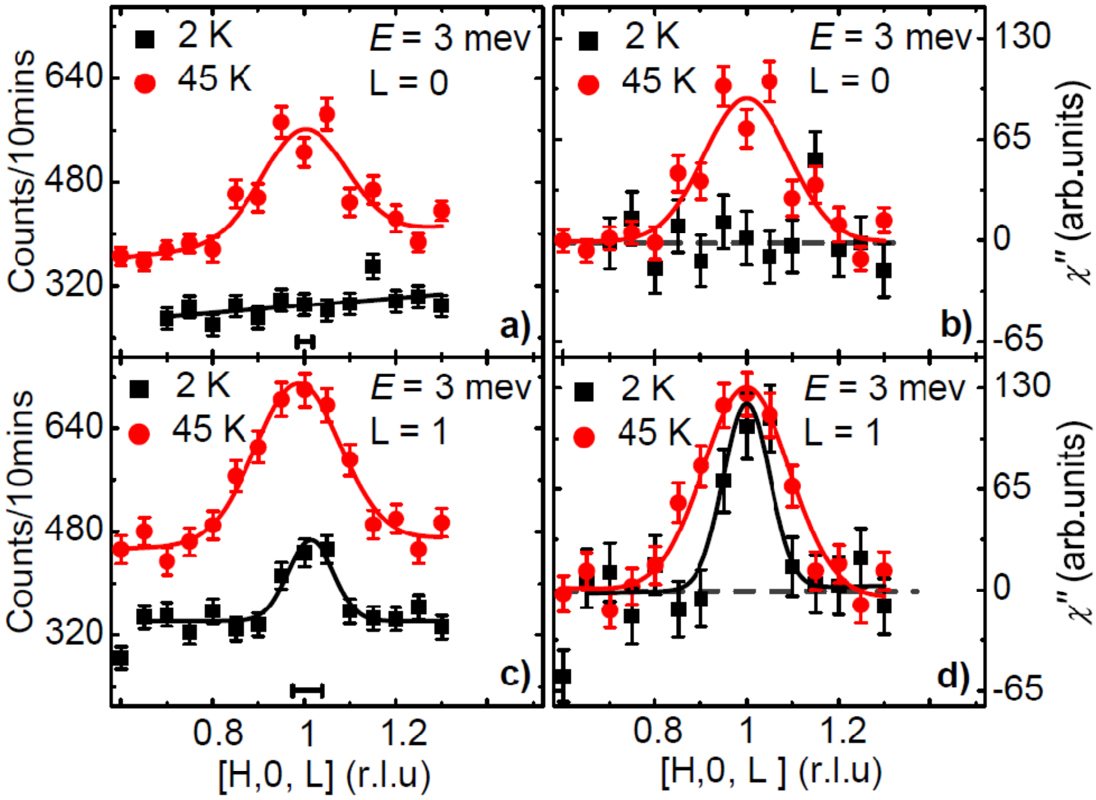

Fig. SI1

Figure SI1 Temperature dependence of the wave vector scans at *E* = 3 meV for $\mathbf{Ba_{0.67}K_{0.33}Fe_2As_2}$. (a-d) show constant energy scans through the (*H*,0,*L*) *L* = odd, even, at temperatures above and below T_c.

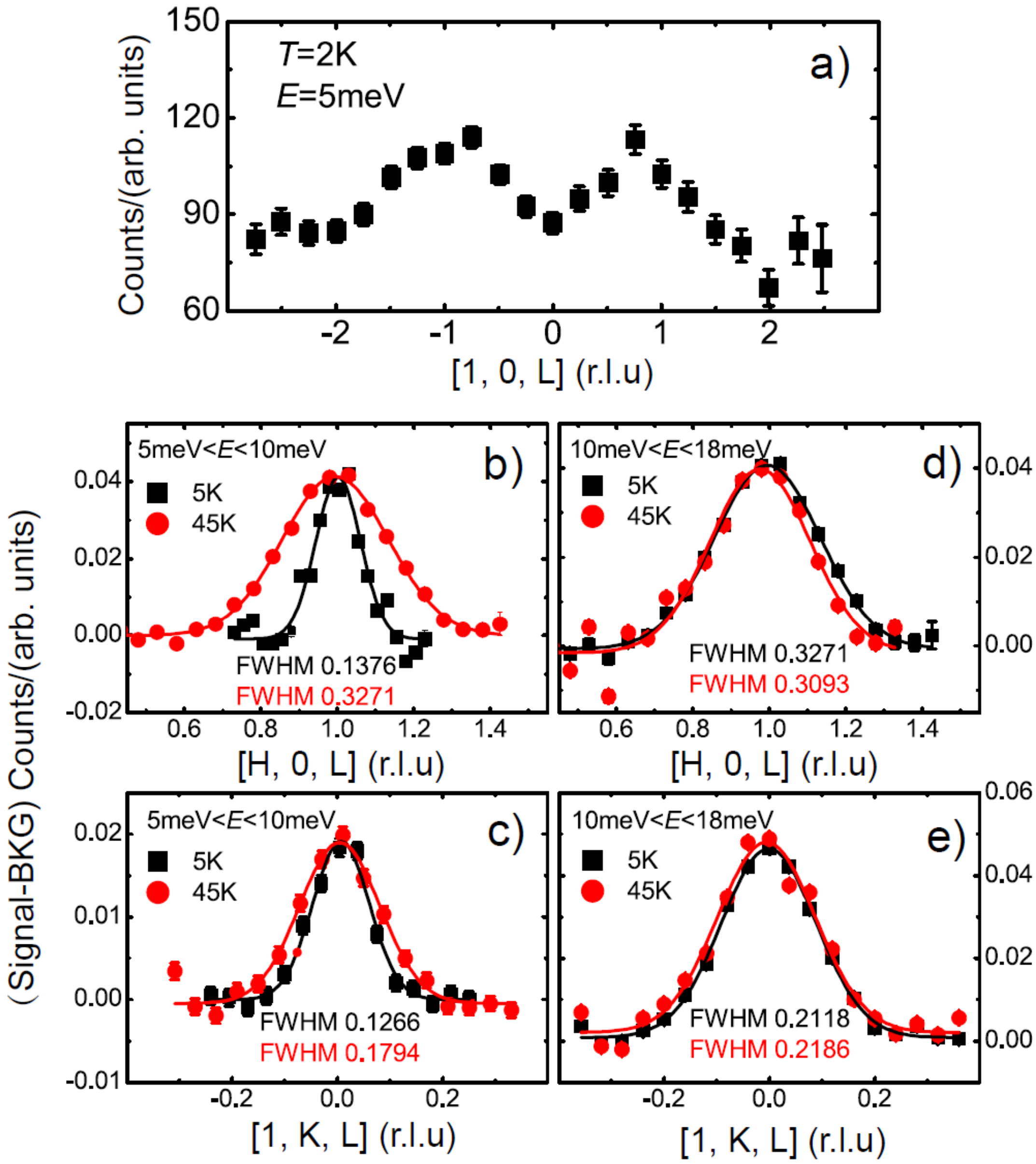

Fig. SI2

Figure SI2 Wave vector and temperature dependence of the magnetic scattering in $Ba_{0.67}K_{0.33}Fe_2As_2$. (a) *Q*-scans at *E* = 5 meV along the (1,0,*L*) directions at 2 K obtained on MACS. The integration range for *H* is from 0.92 to 1.08 rlu. (b-d) are from ARCS. For the *H*-direction cut, the *K*-integration range is from -0.1 to 0.1 rlu. For the *K*-direction cut, the *H*-integration is from 0.85 to 1.15 rlu.

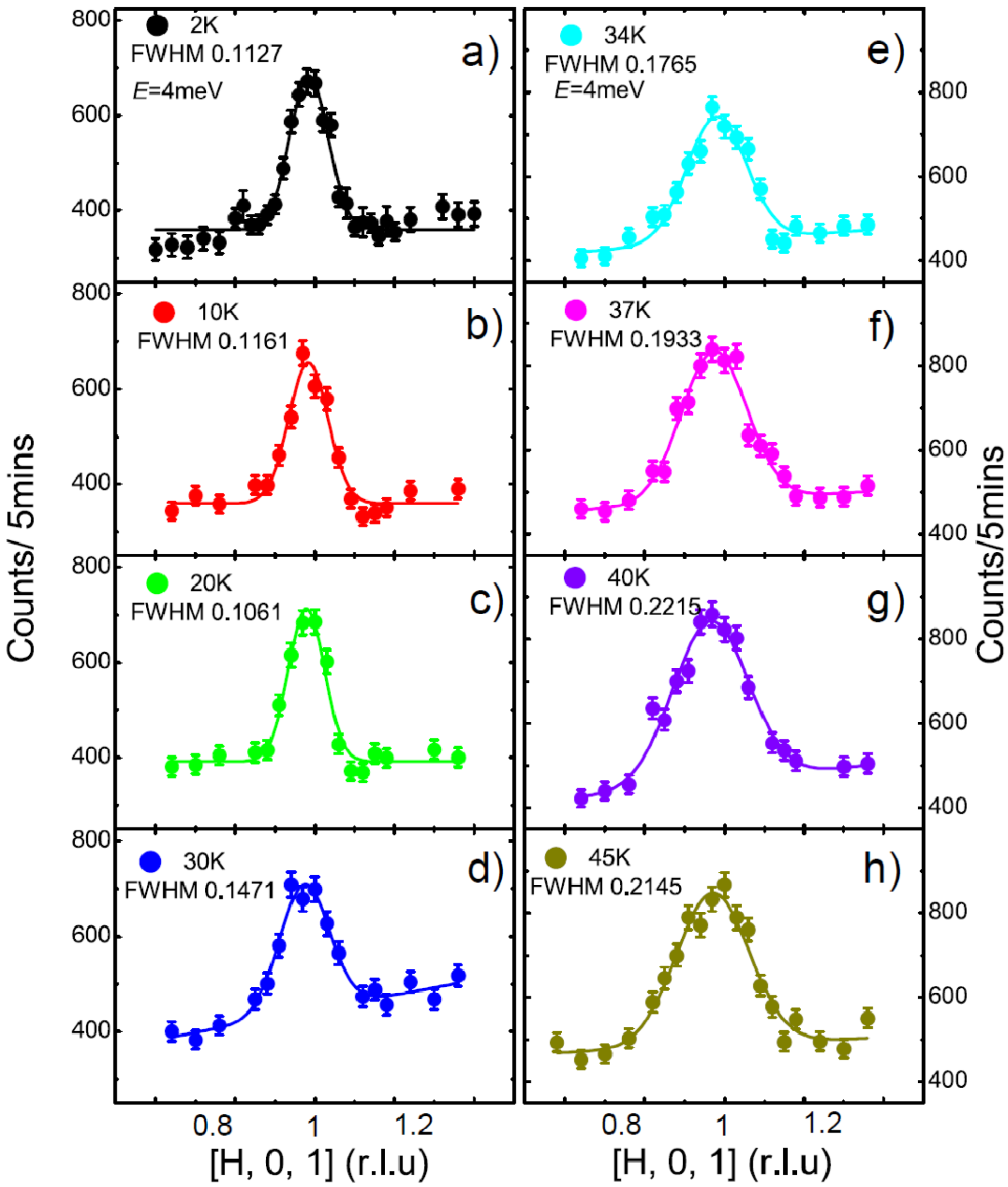

Fig. SI3

Figure SI3 Temperature dependence of the wave vector scans at *E* = 4 meV in $\mathbf{Ba_{0.67}K_{0.33}Fe_2As_2}$. (a-h) Constant energy scans at different temperatures along the (*H*,0,1) direction at E = 4 meV. The full-width-at-half maximum (FWHM) of the Gaussian fits are listed. The data are from MACS.

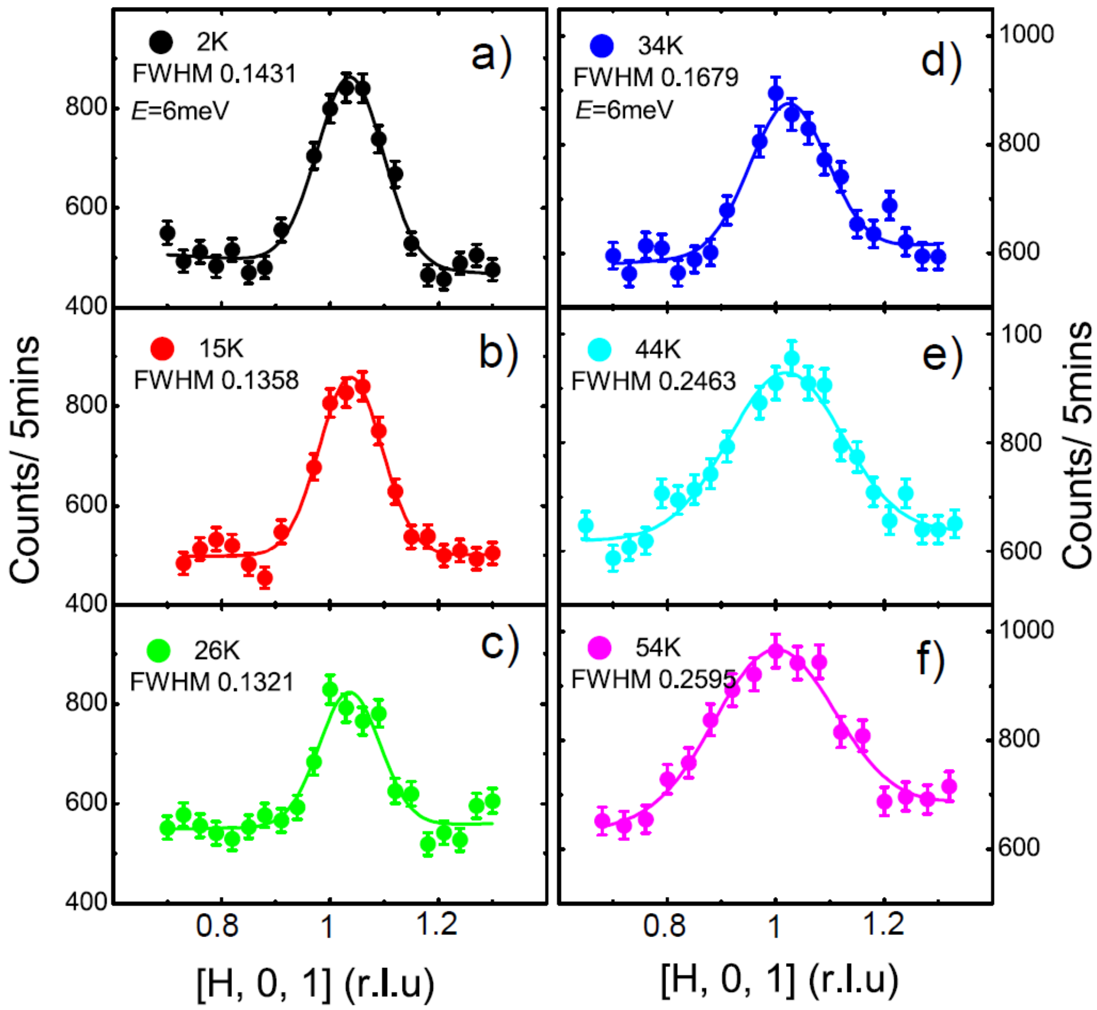

Fig. SI4

Figure SI4 Temperature dependence of the wave vector scans at *E* = 6 meV in $\mathbf{Ba_{0.67}K_{0.33}Fe_2As_2}$. (a-h) Constant energy scans at different temperatures along the (H,0,1) direction at E = 6 meV. The FWHM of the Gaussian fits are listed. The data are from MACS.

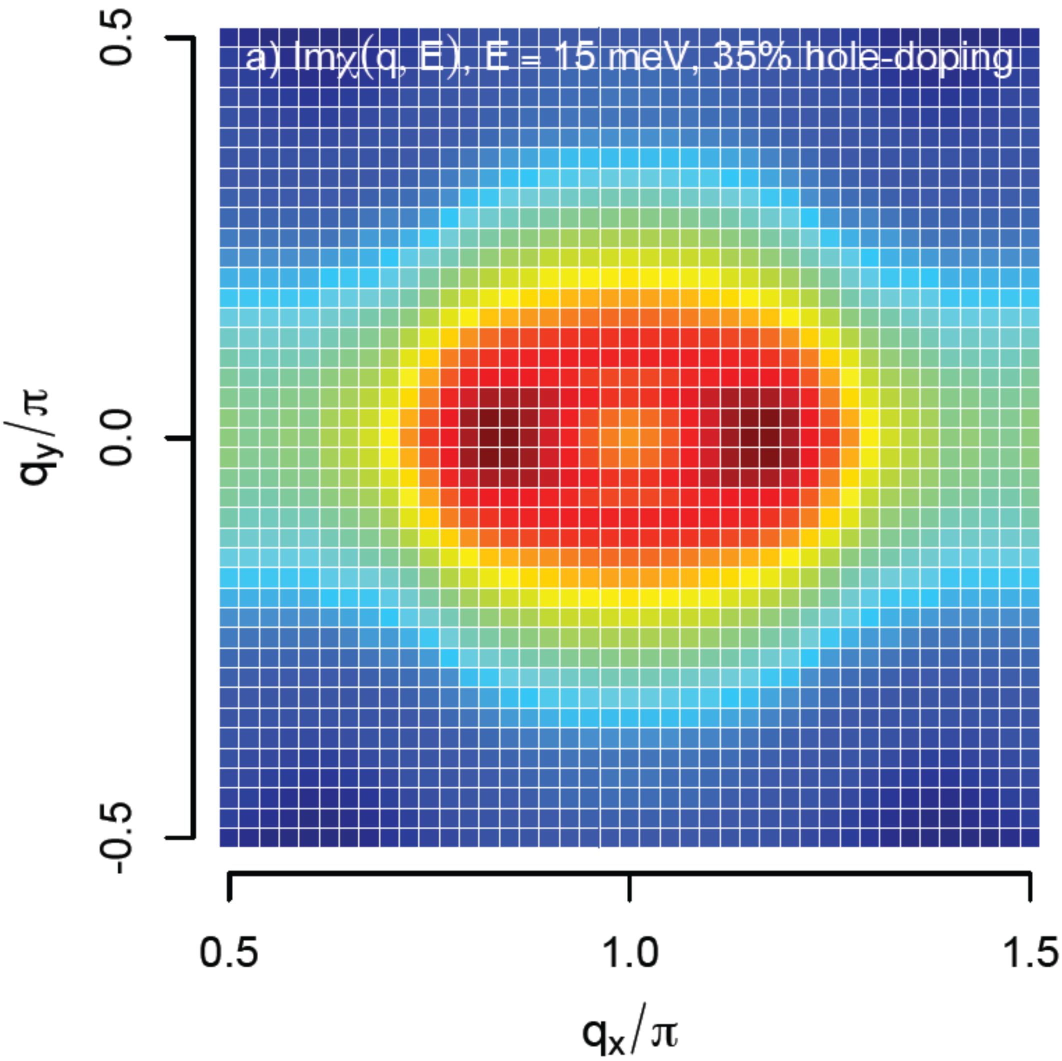

Figure SI5 Imaginary part of the RPA spin susceptibility χ"(Q,ω) for the hole-doped case. The image was calculated from a three-dimensional tight-binding model for fixed energy E = 15 meV as a function of momentum $Q = (Q_x,Q_y,0)$ around $Q_{AFM} = (1,0)$ for a 35% hole-doped case.

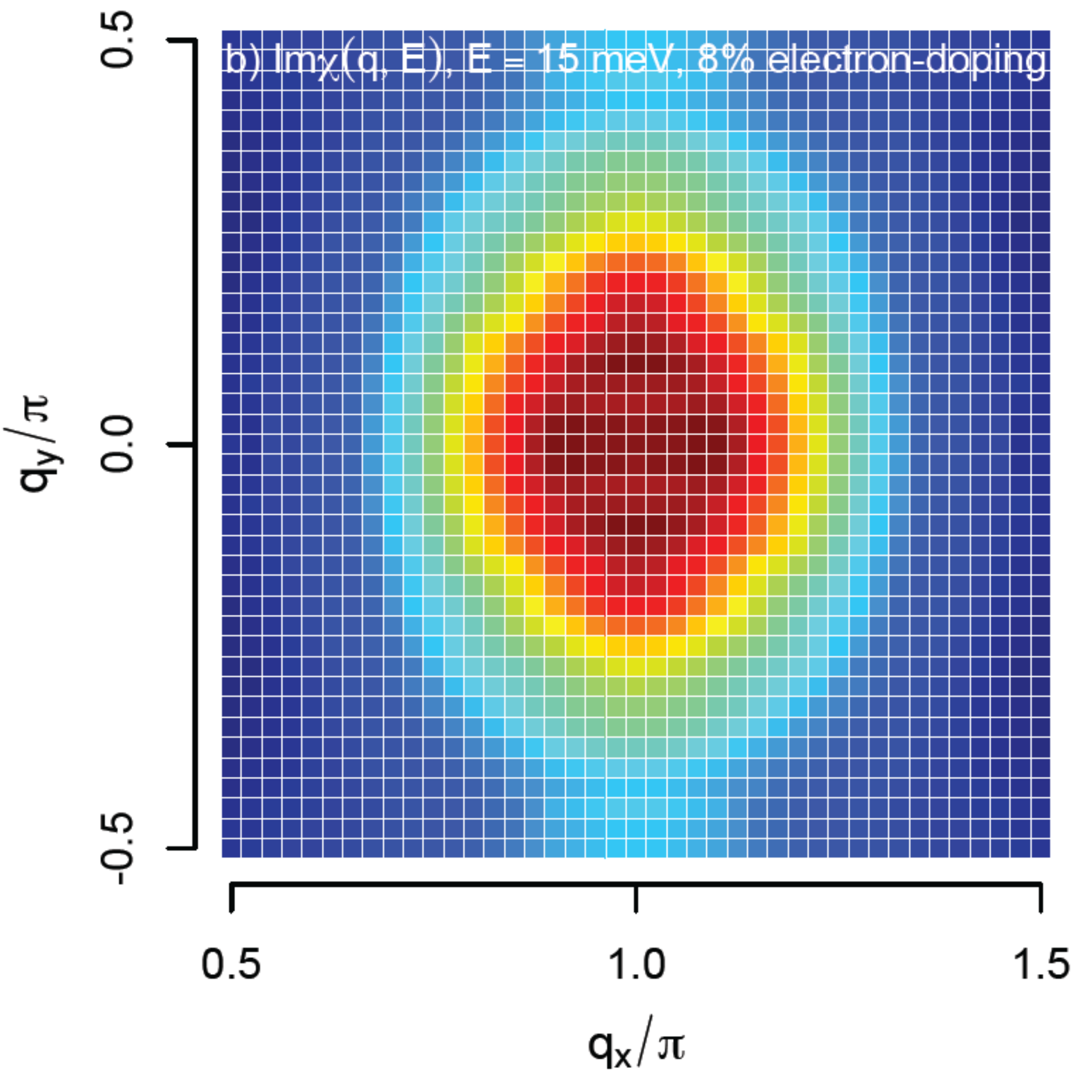

Figure SI6 Imaginary part of the RPA spin susceptibility χ"(Q,ω) for the electron-doped case. The image was calculated from a three-dimensional tight-binding model for fixed energy E = 15 meV as a function of momentum $Q = (Q_x,Q_y,0)$ around $Q_{AFM} = (1,0)$ for an 8% electron-doped case.